Stereoselective Crystallization and Specific Interactions in Polylactides

ARTICLE *in* MACROMOLECULES · AUGUST 2005

Impact Factor: 5.8 · DOI: 10.1021/ma051266z

Stereoselective Crystallization and Specific Interactions in Polylactides

Jose-Ramon Sarasua,* Nerea López Rodríguez, Alberto López Arraiza, and Emilio Meaurio

The School of Engineering, The University of Basque Country (EHU−UPV), Alameda de Urquijo s/n. 48013 Bilbao, Spain

Received June 16, 2005; Revised Manuscript Received July 22, 2005

ABSTRACT: The stereoselective annealing conditions for polylactides to crystallize as α homocrystals (T_m = 180 °C) and/or higher melting temperature (T_m = 230 °C) η stereocomplex crystals are reported in this paper. Differential scanning calorimetry (DSC) and X-ray diffraction (XRD) studies provide evidence of the isothermal annealing conditions in which equimolar mixtures of optically pure poly(L-lactide) and poly(D-lactide) take exclusively the form α, exclusively the form η, or coexist as both α and η crystal polymorphs. Fourier transformed infrared (FTIR) spectroscopy studies reveal a shift to lower wavenumbers in the C=O stretching band of polylactides in the stereocomplex with regard to that in the homocrystal. This band shift is accompanied by similar displacements in the C−H spectral bands. These results are interpreted in terms of H-bonding forces causing specific $CH_3\cdots O{=}C$ and $C_\alpha H\cdots O{=}C$ interactions between both stereoisomers of polylactide. Molecular models support that the suggested hydrogen-bonding arrangement can be accommodated into the stereocomplex crystal lattice. The strength of the interactions has been calculated from both C=O and C−H spectral regions, resulting in a mean value of 1.1 kcal/mol, close to that expected according to ab initio calculations.

Introduction

Polylactides are usually obtained by ring-opening polymerization of lactide, a molecule containing two chiral carbon atoms that provide the possibility of different types of optical activity and crystalline development. One of the most remarkable issues regarding polylactides is its crystal polymorphism. Optically pure polylactides have been reported to crystallize in a pseudo-orthorhombic crystal (α form) with cell parameters a = 1.07 nm, b = 0.595 nm, and c = 2.78 nm.[1,2] However, stereocomplex crystallization has been obtained from equimolar mixtures of poly(L-lactide) and poly(D-lactide).[3] The crystal system is in this case triclinic with cell dimensions a = 0.916 nm, b = 0.916 nm, c = 0.870 nm, α = 109.2°, β = 109.2°, and γ = 109.8°.[2]

Stereocomplexation is a quite rare phenomenon observed in organic polymers. It has been reported to occur by blending tactic polymers of opposite configurations, for example iso- and syndiotactic poly(methyl methacrylate),[4,5] polythiiranes,[6] polyoxiranes,[7] polylactones,[8,9] and more recently polylactides.[2,10] The common feature of all these systems is that crystallization of enantiomeric polymer chains occurs into a crystalline lattice in which chains are more densely packed than in the case of the parent homopolymer crystal lattice. Consequently, enantiomeric polymer blends with stereocomplex crystal structures show higher melting temperatures and different physical and mechanical properties with regard to their parent homopolymers.

Polylactides are biodegradable and bioresobable materials with potential use in repair and regeneration of healing tissues.[11] They also fulfill many requirements of packaging thermoplastics and are therefore considered of great value from an environmental point of view.[12] The versatility of the different polylactide systems based on their particular stereochemistry has generated a great number of referenced studies on polymerization, biodegradation, and physicochemical characterization (crystallization, blending, etc.) that can be found in several recent review articles.[13,14] However, to our knowledge few works have been reported on stereoselective crystallization conditions or specific interactions leading to stereocomplexation in polylactides.[15−18,20]

For example, stereocomplexes of tactic polymers such as PMMA have been studied over decades; however, its structure and driving force for complexation are accepted to be yet a matter of controversy.[19] In the case of polylactides this is even truer. To our knowledege, a work on Raman spectroscopy has been reported[18] providing evidence of the influence of specific interactions on crystallization of polylactide as stereocomplex. A more recent FTIR work by Zhang et al. suggests weak $CH_3\cdots O{=}C$ interactions in the polylactide stereocomplex.[20] In this paper it is provided evidence of the stereoselective crystallization of polylactides by DSC, XRD, and FTIR, together with a discussion on the nature of the specific interactions leading to polylactide stereocomplexation.

Experimental Part

A. Starting Materials. The polylactides used in this study were supplied by PURAC BIOCHEM (Netherlands). Table 1 shows the values of the residual monomer content, the specific rotation in chloroform at 20 °C, the intrinsic viscosity in chloroform at 30 °C, and the viscosimetric molecular weight calculated using the relation[21]

$$[\eta] = 5.45 \times 10^{-4} M_v^{0.73}\ (\mathrm{dL/g}) \qquad (1)$$

B. Film Preparation. PLLA and PDLA pellets were dried in a vacuum oven at 60 °C overnight. Both PLLA and PDLA dissolve in chloroform and remain stable at room temperature. Polylactide films were obtained from 2 wt % solutions in chloroform. Films of PLLA, PDLA, and their 1:1 blend based on weight (this is the equimolar mixture of both optically pure opposite isomers), hereafter named B-5050, were prepared by

* Corresponding author. E-mail: joseramon.sarasua@ehu.es.

10.1021/ma051266z CCC: $30.25
Published on Web 08/24/2005

Table 1. Characteristics of Polylactides[a]

material	RS (%)	RM (%)	α (deg)	[η] (dL/g)	M_v (g/mol)
PLLA	<0.01	<0.1	−157.3	5.74	3.23×10^3
PDLA	<0.03	<0.2	+158.2	5.68	3.19×10^3

[a] RS = residual solvent; RM = residual monomer; α = rotatory power in $CHCl_3$ at 25 °C; [η] = intrinsic viscosity; M_v = molecular weight (viscometric).

casting the polylactide solutions into Petri dishes. After preparation the films were dried for at least 24 h into a vacuum oven at 60 °C to ensure complete evaporation of the solvent. The dried films were stored in the presence of silica gel to avoid moisture absorption until annealing and/or characterization was carried out.

C. Annealing of Samples. Annealing of the stoichiometric blends of the optically pure poly(L-lactide) and poly(D-lactide) was conducted in an oven at 140, 150, 160, 170, 180, and 190 °C in order to study the crystalline evolution behavior (type of polymorph and amount developed) of polylactides during annealing. The specimens were withdrawn at regular intervals and stored in the presence of silica gel until the characterization was conducted by DSC and/or XRD.

D. Differential Scanning Calorimetry. Thermal analysis of the films both as obtained and annealed at several temperatures and times was carried out on a DSC from TA Instruments, model DSC 2920. Approximately 5 mg of each material was weighted and sealed in an aluminum pan. The crystallization and melting behavior was determined during the first scan at 20 °C/min.

E. X-ray Diffraction. X-ray diffraction of films was carried out in a Philips PW 1820 apparatus with automatic acquisition of data each 0.050°. Diffraction angles reported are for Cu α radiation (λ = 1.542 Å).

F. Infrared Spectroscopy. Infrared spectra of blends were recorded on a Nicolet AVATAR 370 Fourier transform infrared spectrophotometer (FTIR). Spectra were taken with a resolution of 2 cm^{-1} and were averaged over 64 scans. Chloroform solutions containing 0.5 wt % polylactide were cast on KBr pellets, and samples were vacuum-dried at 60 °C for 48 h. The absorbance of all the studied samples was within the absorbance range in which the Lambert−Beer law is obeyed. Second-derivative spectra were smoothed with a quartic 11-point Savitzky−Golay smoothing filter.[22] Corrected coefficients are found in ref 23. The degree of distortion of this smoothing algorithm was checked by the procedure specified in a previous paper.[24]

The spectra of blends B-5050 were recorded after melting at 240 °C and cooling to the isothermal crystallization temperature selected, 190 °C. This temperature was chosen because it ensures the stereoselective crystallization of the polylactide exclusively in the stereocomplex η form since the α crystalline polylactide melts at 180 °C. On the other hand, FTIR spectra of PLLA were recorded after melting at 200 °C and cooling the samples to the isothermal crystallization temperature of 150 °C in which polylactide α crystals develop.

G. Molecular Modeling. Bond lengths and angles of the RIS model have been transferred from literature and are based on results obtained in structural analysis of esters and the accepted standard values of these parameters in organic molecules.[39,40] The 3D structure has been built with the free software package Arguslab 4.0.1.[56]

Results and Discussion

DSC Analysis. Polylactides show a low melting temperature peak at about 180 °C, corresponding to the fusion of homocrystals of optically pure samples, and a higher melting temperature peak at about 230 °C, corresponding to the stereocomplex crystal fusion in blends of the two optically pure enantiomers of polylactide.[25,26,28] The DSC traces of as-cast PLLA and the stoichiometric blend B-5050 are shown in Figure 1. Both exhibit the typical exotherm corresponding to the cold crystallization and the endotherm corresponding to the fusion of crystals. In the case of B-5050 there is a double endothermic peak that is attributed to the presence of a population of α homocrystals melting at about 180 °C and a population of η stereocomplex crystals melting at about 230 °C.

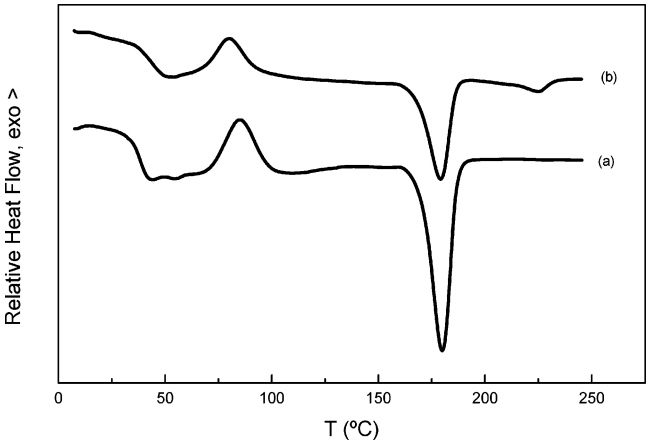

Figure 1. DSC curves of as-cast PLLA (a) and as-cast PLLA/PDLA B-5050 stoichiometric blend (b).

Table 2. Melting Enthalpies of Homocrystals (ΔH_H) and Stereocomplex Crystals (ΔH_S) and Overall Crystallinities Calculated Using ΔH_H^0 = 106 J/g and ΔH_S^0 = 142 J/g (Ref 28)

	annealing time					
	1 h			24 h		
annealing T (°C)	ΔH_H (J/g)	ΔH_S (J/g)	X_c (%)	ΔH_H (J/g)	ΔH_S (J/g)	X_c (%)
140	24.22	1.86	24.03	24.70	0.97	23.92
150	31.90	2.01	31.35	38.18	1.58	36.99
160	33.01	2.17	32.51	39.32	2.28	38.52
170	38.29	2.05	37.42	45.97	3.90	45.82
180	39.21	1.16	37.73	41.09	10.47	45.50
190	22.44	22.64	40.04		87.28	61.46

The crystalline amount of semicrystalline polymers depends on thermal treatments carried out on samples. In another study we demonstrated that the relative amount of stereocomplex vs homocrystal formation in polylactide enantiomeric blends was favored under nonisothermal crystallizations carried out at low cooling rates from the melt.[28] Aimed at defining more accurately the thermal conditions under which the selective crystallization of the forms α and η can be accomplished in polylactide enantiomeric blends, annealing treatments were carried out at 140, 150, 160, 170, 180, and 190 °C. Table 2 shows the values of the melting enthalpy of homocrystals and stereocomplex crystals obtained by DSC after annealing the B-5050 sample for 1 and 24 h at these temperatures. As can be seen, for samples annealed for 1 h at temperatures below 180 °C, the melting enthalpy of homocrystals is much larger than the melting enthalpy of stereocomplex crystals, indicating that the α crystal polymorph formation is favored at these conditions. For 24 h annealing the situation is quite similar; in this case the overall crystallinity degree of the samples is slightly increased, and the melting enthalpy values indicate that the relative amount of the α type crystals vs stereocomplex crystals developed at these conditions is high. This relative amount of α vs η type crystals is approximately the same, remaining above 90% for 1 h and 24 h annealing times at temperatures lower than 180 °C.

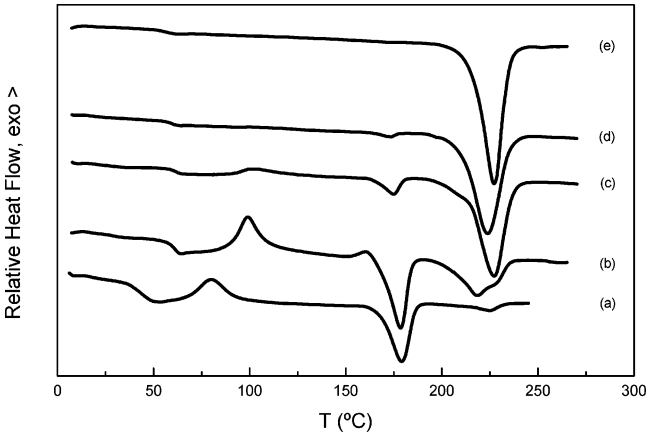

Figure 2. DSC curves of stoichiometric PLLA/PDLA blends: as-cast (a) and after annealing at 190 °C for 1 (b), 4 (c), 8 (d), and 24 h (e).

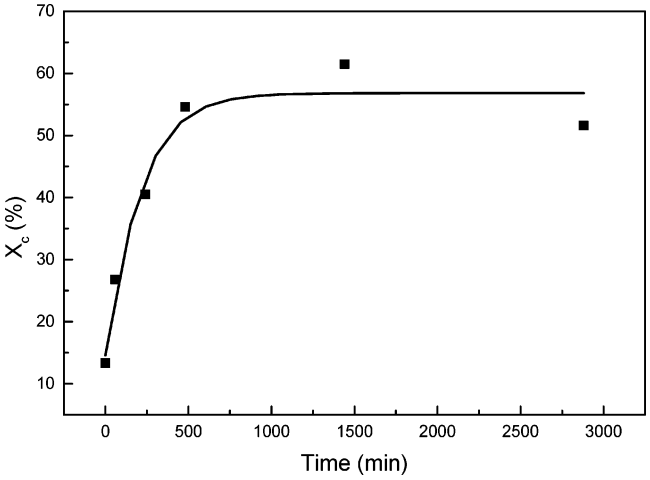

Figure 3. Evolution of overall crystallinity (X_c) with annealing time for stoichiometric PLLA/PDLA blends annealed at 190 °C. X_c values were calculated according to ref 28.

However, when annealing temperature reaches the melting temperature of α crystals (please note that the melting endotherm in the DSC trace of α homocrystallites begins at 170 °C and finishes at about 190 °C), the crystal type formation is drastically inversed. For 1 h annealing at 190 °C the relative amount of stereocomplex crystallization reaches 50% and attains nearly the 100% value for 8 h annealing. These values indicate that the α crystals of polylactide, when remelting at 190 °C during annealing, recrystallize selectively as a stereocomplex.

The annealing for several hours at 190 °C is probably a harsh condition for a thermally unstable polylactide. To evaluate the possible thermal degradation during annealing at 190 °C, viscometric measurements were carried out at 30 °C with dilute solutions of the annealed films in chloroform. The results showed a decrease of the molecular weight with annealing time, reaching a 27% loss of its initial value after 8 h annealing. Films annealed for longer times were not tested because they hardly dissolved in chloroform. These results lead to the conclusion that some degradation is taking place during annealing and that it is plausible that a decrease in the molecular weight may be favoring the stereocomplexation process in polylactides.

The recrystallization kinetics of B-5050 at 190 °C was also followed by DSC. Figure 2 shows the DSC traces of the stoichiometric blend, as-cast and after 1, 4, 8, and 24 h annealing at 190 °C. All curves, except the as-cast sample that shows a smaller value attributed to some plasticization due to solvent, show the typical T_g value of polylactide at about 60 °C. In addition, typical cold crystallization behavior is observed for annealing times shorter than 4 h. Higher annealing times imply no cold crystallization. Interestingly, an inversion of the relative melting peak areas is found at about 4 h annealing, indicating that for larger annealing times the amount of stereocomplex crystals exceeds that of α homocrystallite. Finally, 24 h annealing is needed to attain 100% stereocomplex crystallization. It must be emphasized that this value does not correspond to the full crystallization of the sample but only to the 100% stereocomplex formation of the crystalline phase of a partly amorphous polylactide. The evolution of overall crystalliny of B-5050 at 190 °C with annealing is reported in Figure 3.

X-ray Diffraction. X-ray diffraction is an accurate experimental technique with which crystalline polymorphs of polylactide can be elucidated. It has been reported that a highly crystalline sample of α polymorph of optically pure PLLA showed its most intense diffraction peaks at 2θ values of 14.5°, 16.3°, 18.7°, and 21.9°.[27] The crystalline lattice of the α polymorph of polylactides is reported to be pseudo-orthorhombic and contains two 10_3 helices.[3] However, the diffraction pattern of the PLLA/PDLA blends crystallized as stereocomplex is very different from that of the optically pure polylactides crystallized as α polymorph and presents three main diffraction peaks at 2θ equal to 12°, 21°, and 24°.[2,3,27] The stereocomplex crystallizes in a triclinic system in which L-lactide and D-lactide segments are packed parallel taking a 3_1 helical conformation. Since a β polymorph (PLLA stretched fibers and drawn films)[29−31] and a γ polymorph (epitaxial crystallization of PLLA on hexamethylbenzene)[32] have also been reported for optically pure polylactides, in this work the stereocomplex crystal form has been named η, to avoid any confusion with the above-mentioned β form observed in stretched optically pure polylactide fiber and films.

Figure 4 shows the X-ray diffraction patterns of optically pure PLLA (bottom) and of the equimolar mixture of optically pures poly(L-lactide) and poly(D-lactide) (PLLA/PDLA) after crystallizations at different annealing conditions. Optically pure nonblended PLLA, crystallized 24 h at 140 °C, shows its most intense peak at a 2θ = 16.6° due to reflections from (200) and/or (110) planes. Less intense peaks are also observed at 2θ = 14.7°, 18.9°, and 22.1°, corresponding respectively to reflections of (010), (203), and (015) planes. These results are in close agreement with the peaks reported in the literature for the α polymorph. The stoichiometric blend of optically pure poly(L-lactide) and poly(D-lactide), crystallized 24 h at 140 °C, showed a very similar pattern of that of PLLA, with the most intense peaks at 2θ values of 14.7°, 16.6°, and 22.1° due to reflections of (010), (200), and/or (110) and (015) planes, indicating a quasi-exclusive crystallization in the form α (a small diffraction peak at 12° suggests the presence of a small quantity of the η polymorph). In contrast, the stoichiometric blend annealed at 190 °C showed a very different X-ray pattern. In the case of the 1 h annealed sample the most intense diffraction peaks reveal that both α (peak at 16.6°) and η polymorphs (peaks at 12°, 21°, and 24° due to reflections of (101), (204), and (211) planes) are present. It is also to be noted that very close to the

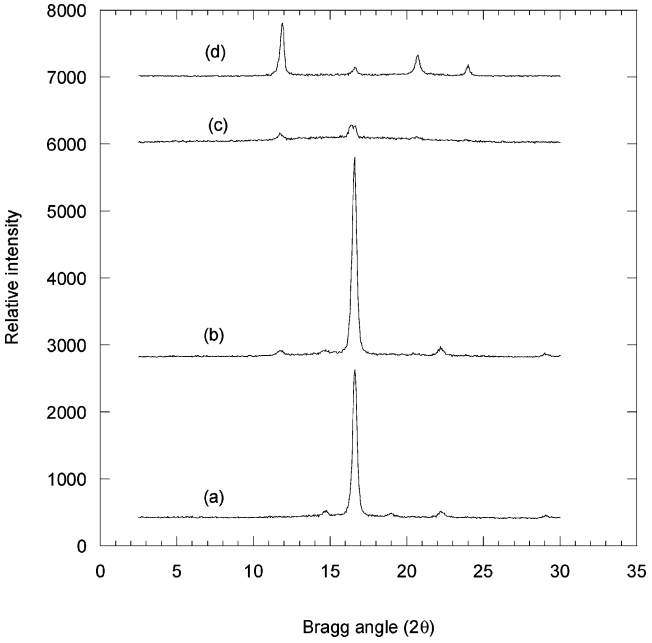

Figure 4. X-ray diffraction curves of PLLA annealed at 140 °C for 24 h (a) and of PLLA/PDLA B-5050 stoichiometric blend annealed at 140 °C for 24 h (b), at 190 °C for 1 h (c), and at 190 °C for 24 h (d).

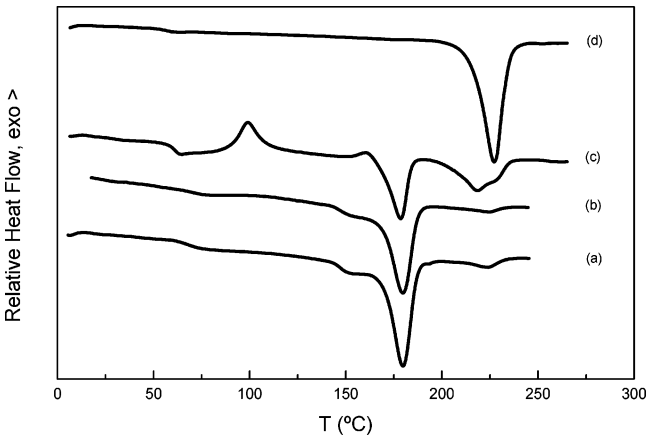

Figure 5. DSC curves of stoichiometric PLLA/PDLA blends submitted to different annealing conditions: (a) 140 °C, 1 h; (b) 140 °C, 24 h; (c) 190 °C, 1 h; (d) 190 °C, 24 h.

16.6° peak attributed to reflections of the α crystal appears a peak at 16.4° that is attributed to (110) reflections of the stereocomplex crystal.[16] For the 24 h annealed stoichiometric blend, the peak at 16.6° disappears and the most intense peaks appear at 12°, 16.4°, 21°, and 24°, indicating that the stereoselective crystallization in the form of stereocomplex has been achieved.

The evolution of the stereoselective crystallization of the equimolar blends has been studied by DSC in the same annealing conditions used for X-ray diffraction (see Figure 5). The 140 °C annealed sample (annealing time 24 h) shows a large endothermic peak centered at about 180 °C, corresponding to the fusion of a population of α crystals indicating quasi-exclusive crystallization in this crystal polymorph. (In this case only a very small endotherm centered at about 230 °C is observed, indicating the fusion of a very small quantity of stereocomplex crystals.) In contrast, the 190 °C annealed samples show a different behavior. For 1 h annealing double melting behavior is observed, indicating that both α and η polymorphs are present. Finally for 24 h annealing at 190 °C, the melting endotherm corresponds exclusively to the fusion of stereocomplex crystals. These results are in agreement with X-ray diffraction patterns studied above and evidence the temperature dependence of stereoselective crystallization of polylactides.

FTIR Analysis. Stereocomplexation hardly develops when mixing high molecular weight stereoisomers, a result related to the smaller overall mobility of high molecular weight chains compared to that of the lower molecular weight ones.[33] The overall spectral features of polylactides have been reported in recent studies,[17,20,34−38] but important aspects, such as the specific interactions responsible for the unusual phase transformations observed in these systems, remain obscure. In a parallel paper,[39] the crystallization of PLLA was studied by our group from the spectral changes observed in the C=O stretching and in the C−O−C asymmetric stretching regions. Unusually complex behavior was observed in the carbonyl stretching region, successfully explained in terms of mechanical coupling between C=O groups along the chain. A study of the crystallization behavior of the stereocomplex should take into account these findings for a correct interpretation of the observed spectral changes because obviously mechanical coupling is also expected.

The IR spectrum of PLLA was found to exhibit conformational sensitivity.[39] According to the conformational analysis of PLLA,[40] three skeletal bonds occur along the molecular chain in poly(lactic acid): C−O (ester), O−C_α, and C_α−C. The C−O (ester) bond is assumed to be always trans due to conjugation with the C=O double bond. The O−C_α bond has two energy minima around −160° and −48°, and the C_α−C bond has two energy minima around 160° and −73°. Since 160° is close to 180°, the 160° angles are termed trans (t). In the same way, −48° and −73° are close to −60° and are termed gauche (g+). The analysis of PLLA predicts four minimum-energy states corresponding to four distinct conformations for the O−C_α and C_α−C bonds: tt (−160°, 160°), tg (−160°, −48°), gt (−73°, 160°), and gg (−73°, −48°). In the case of PDLA, dihedral angles obtained for the minima have identical value but opposite sign. Hence, PDLA chains adopt specular conformations; for example, the 3_1 helix in PLLA is left-handed, but the same helix in PDLA is right-handed. Nevertheless, both helixes are identical from a spectroscopic point of view.

The analysis of the C=O stretching region of crystalline PLLA[39] allowed the identification of bands attributed to the different conformers predicted by Tonelli et al.[40] It was possible to resolve individual components due to the combination of the following factors:[39] (i) Mechanical coupling between C=O groups generates different normal modes that can absorb at wavenumbers in the range between the in-phase and the out-of-phase mode, separated by about 28 cm^{-1} in polylactides. (ii) The particular conformation of the PLLA chain selects the wavenumber at which absorption occurs. In the case of PLLA, the four possible conformers exhibit single absorption bands, spaced by about 9 cm^{-1} from each other. (iii) Last, crystallization was observed to promote a semiordered interphase material, characterized by narrow bands of about 9 cm^{-1}. Hence, the individual bands assigned to the different conformers are spaced by about their half-height width, a condition usually accepted to give appropriate spectral resolution.

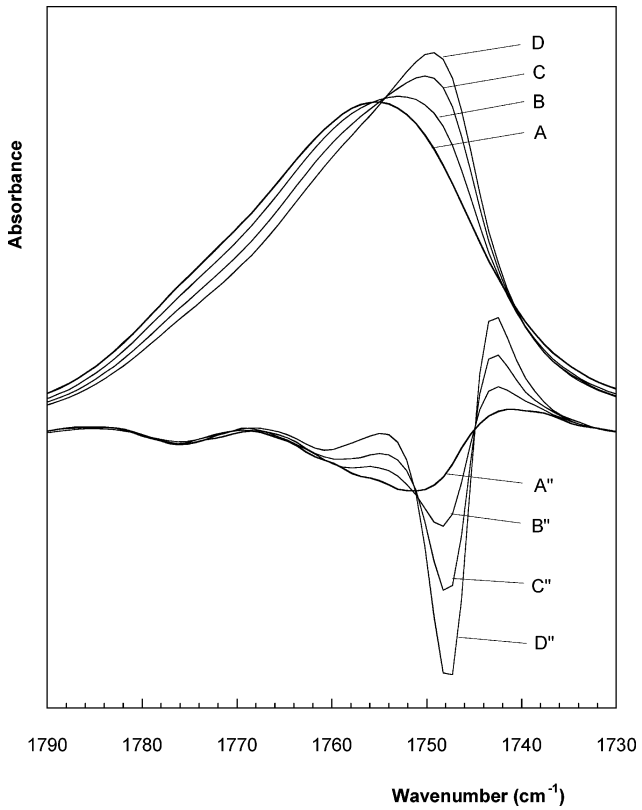

Figure 6. Carbonyl stretching region of B50-50 (upper side spectra) and second derivatives (bottom side spectra) recorded during isothermal crystallization at 190 °C, after melting at 240 °C: (A) 0 min (amorphous blend); (B) after 4 min; (C) after 30 min; (D) after 8 h.

Table 3. Effect of Annealing Temperature and Time in Stereocomplex Crystal Formation; $X_{stereocomplex} = [\Delta H_S/(\Delta H_H + \Delta H_S)] \times 100$

	$X_{stereocomplex}$ (%)	
annealing T (°C)	1 h	24 h
140	7.1	3.8
150	5.9	3.9
160	6.2	5.5
170	5.1	7.8
180	2.9	20.3
190	50.2	100

Table 4. Conformer Population Distribution at Different Temperatures; Absorption Band Locations in the C=O Stretching Region Are Also Included

conformer	location (cm^{-1})	population % at 30 °C	population % at 150 °C	population % at 190 °C
gg	1776	18.2	19.0	18.9
tg	1767	6.8	7.7	8.8
gt	1759	47.4	41.4	38.3
tt	1749	27.6	32.0	33.9

C=O Spectral Region. Figure 6 shows the spectra obtained for the isothermal crystallization of the stoichiometric blend, B50-50, at 190 °C, after melting for 2 min at 240 °C. As expected, the second derivative of amorphous B50-50 is identical to that reported for neat PLLA,[39] showing two broad bands at 1776 and 1755 cm^{-1}. Splitting of this spectral band is attributed to conformational sensitivity. The conformer population distribution at 150 °C along with the corresponding band locations is reported in Table 4. As can be seen, gt, tt, and gg are dominant conformers, and the band at 1755 cm^{-1} can be attributed to the overlapping contributions from gt and tt conformers, while the band at 1776 cm^{-1} is attributed to gg conformers. During crystallization, a new peak at 1748 cm^{-1} gains intensity, attributed to crystalline B50-50 in the 3_1 helix conformation.[16] The other two second-derivative bands are located at 1776 and 1760 cm^{-1} and can be attributed to the amorphous phase. The shape of these second-derivative bands does not change during crystallization, and the shift observed from 1755 to 1760 cm^{-1} for the lower wavenumber amorphous band can be reasonably attributed to the overlap of this low-intensity band with the negative side lobe of the high-intensity crystalline peak. These results indicate that polymer chains in the interlamellar region remain in the random conformation characteristic of the amorphous phase. This behavior differs from that exhibited by neat PLLA, where narrow bands resulting from the crystallization process were attributed to the contributions of the individual conformers in a semiordered interphase.[39] Hence, the crystallization mechanism of PLLA appears completely different than that of B50-50.

The absorption location of the C=O group in the stereocomplex can be compared to the value expected for a polylactide in 3_1 helical conformation. Carbonyl groups in helical chains can display two absorption bands: one attributed to the A mode (transition moment parallel to helix axis) and one attributed to the E mode (transition moment perpendicular to helix axis).[34,39] The A mode absorption was discarded because C=O groups are nearly perpendicular to helical chain.[39] Hence, the band at 1748 cm^{-1} must be attributed to the E mode, so that the phase angle between coupled C=O groups for absorption to occur is

$$\phi = \frac{2\pi a}{H} \tag{2}$$

where H is the number of monomer units and a is the number of turns, resulting in a value $\phi = 120°$ for a 3_1 helix. In the study of crystallization of PLLA, coupling between C=O groups was observed to split the absorption location for the carbonyl peak according to the following dispersion curve equation:[39]

$$\nu^2 = \nu_0^2 + 2\nu_0\Delta\nu \cos\phi \tag{3}$$

where ϕ is the phase angle for the coupled normal mode for which absorption is expected according to symmetry rules, ν is the absorption frequency, ν_0 is the absorption frequency for the uncoupled C=O group, and $\Delta\nu$ is the frequency difference between the uncoupled mode and the in-phase ($\phi = 0°$) or out-of-phase ($\phi = 180°$) modes. Obtained values for ν_0 and $\Delta\nu$ are respectively 1763 and 14.0 cm^{-1};[39] hence, the absorption wavenumber predicted from eq 2 for a polylactide in a 3_1 helix is 1756 cm^{-1}. The experimental value, 1748 cm^{-1}, indicates a shift of 8 cm^{-1} to lower wavenumbers for the C=O absorption peak of the stereocomplex.

There are two possible reasons to explain this moderate shift: dipole−dipole coupling interaction between ester groups in an ordered structure[41] and the interaction between C=O and C−H bonds.[42−44] Dipole−dipole coupling has been discarded by Tsuji et al.,[20] based on the similarity of the infrared and Raman spectra. To confirm the occurrence of hydrogen bonds in the stereocomplex, it is necessary to inspect the C−H spectral region.

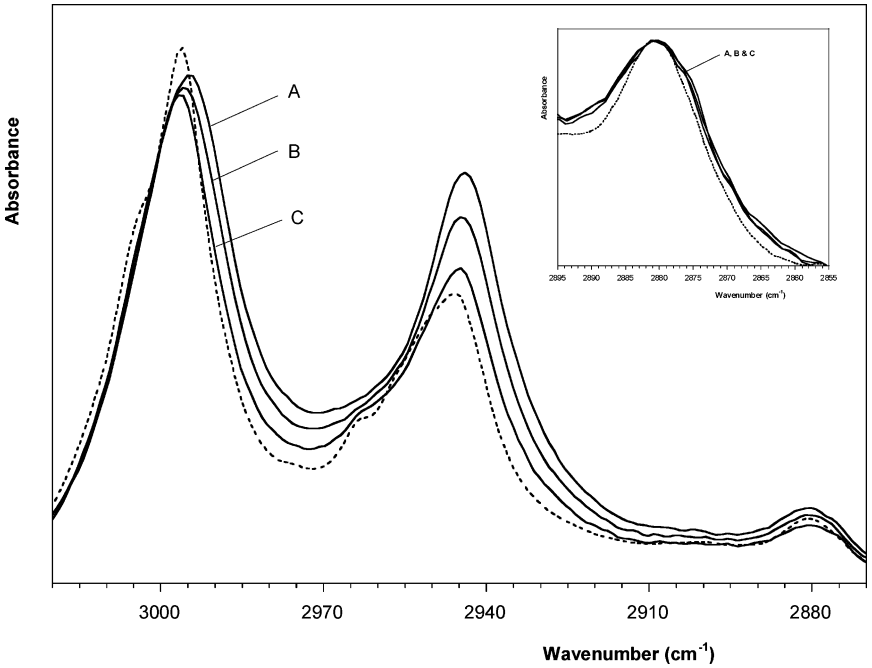

Figure 7. C−H stretching region of PLLA recorded during isothermal crystallization at 150 °C, after melting at 200 °C for 2 min: (A) 0 min (amorphous PLLA); (B) after 7 min; (C) after 70 min. The spectrum obtained at room temperature after crystallization is highlighted with a dotted line. The autoscaled C_α−H stretching region is shown in the upper side square.

Table 5. Peak Locations Obtained from Band Maxima in the C−H Stretching Spectral Region at Room Temperature

	peak location (cm^{-1})		
sample	$\nu(C_\alpha H)$	$\nu_s(CH_3)$	$\nu_{as}(CH_3)$
amorphous PLLA	2880	2945	2995
crystalline PLLA	2880	2946	2996[a]
estereocomplex	2876	2941	2990[b]

[a] Fundamental modes located at 2996 and 3005 cm^{-1}, according to second-derivative analysis. [b] Fundamental modes located at 2989 and 2995 cm^{-1}, according to second-derivative analysis.

C−H Spectral Region. For a correct discrimination of the spectral changes attributable to the crystallization process of B50-50, the changes observed in the neat polymer should be contemplated. Hence, we will first briefly discuss this spectral region for PLLA (Figure 7). Its profile is quite simple, and bands at 2995, 2944, and 2880 cm^{-1} can be assigned respectively to the CH_3 asymmetric stretching, CH_3 symmetric stretching, and C_α−H stretching modes.[34] However, some complicating factors should also be also considered. The band at 2995 cm^{-1} is in fact the overlapping profile of two nearly degenerate fundamental asymmetric modes,[45,46] and the symmetric CH_3 stretch normally can have strong mixing with the overtones of the CH_3 asymmetric deformation modes.[38,46]

Changes observed in the C−H stretching region of neat PLLA during isothermal crystallization at 150 °C after melting at 200 °C are also shown in Figure 7. The CH_3 stretching peaks shift slightly to higher wavenumbers during the ordering process (about 1 cm^{-1}, see Table 5), while the C_α−H stretching peak remains unchanged. Cooling to room temperature does not involve any additional shift. Such small spectral changes suggest that crystallization does not promote C−H···O hydrogen bonding to any measurable extent. Figure 7 displays an additional interesting feature: in amorphous PLLA, a single band appears in the CH_3 symmetric stretching region, but as crystallization proceeds, new bands are observed highly overlapped with the $\nu_s(CH_3)$ band. These bands are attributed to Fermi resonance between the symmetric methyl stretch fundamental and the overtones of the methyl asymmetric bending modes, which appear near 1455 cm^{-1},[46] indicating lateral chain−chain interaction. As can be observed, the intensity of these bands increases during crystallization, but the intensity enhancement is even higher during cooling to room temperature. Both the shift of the CH_3 stretching bands to higher wavenumbers and the presence of Fermi resonance indicate certain lateral interchain interaction among CH_3 groups. It is difficult to assign this interaction to the crystalline phase, the interphase, or both.[47] Finally, cooling to room temperature sharpens the resolution of the two asymmetric CH_3 fundamental modes, located at 2996 and 3005 cm^{-1} according to second-derivative analysis. This frequency difference is similar to that observed in *n*-alkanes,[46] 10 cm^{-1}.

On the other hand, when B50-50 crystallizes, notable spectral changes are observed. Figure 8 shows the changes observed in the C−H stretching region of B50-50 during isothermal crystallization at 190 °C, after melting for 2 min at 240 °C. The spectrum recorded after cooling to room temperature is also displayed. During the isothermal crystallization step, in the CH_3 stretching region, the asymmetric peak is intensified and the area of the symmetric peak decreases, but both bands shift about 2 cm^{-1} to lower wavenumbers. In addition, the red shift increases during cooling to room temperature, resulting in a total value of about 4 cm^{-1} (see Table 5). The occurrence of red shifts in C−H···O=C hydrogen bonds is typically related to the existence of weak to moderate hydrogen bonds,[42−45] in agreement with the spectral shift observed for the carbonyl stretching region. Thus, spectral results suggest that crystallization of the stereocomplex is accompanied by the occurrence of both CH_3···O=C and $C_\alpha H$···O=C hydrogen bonds.

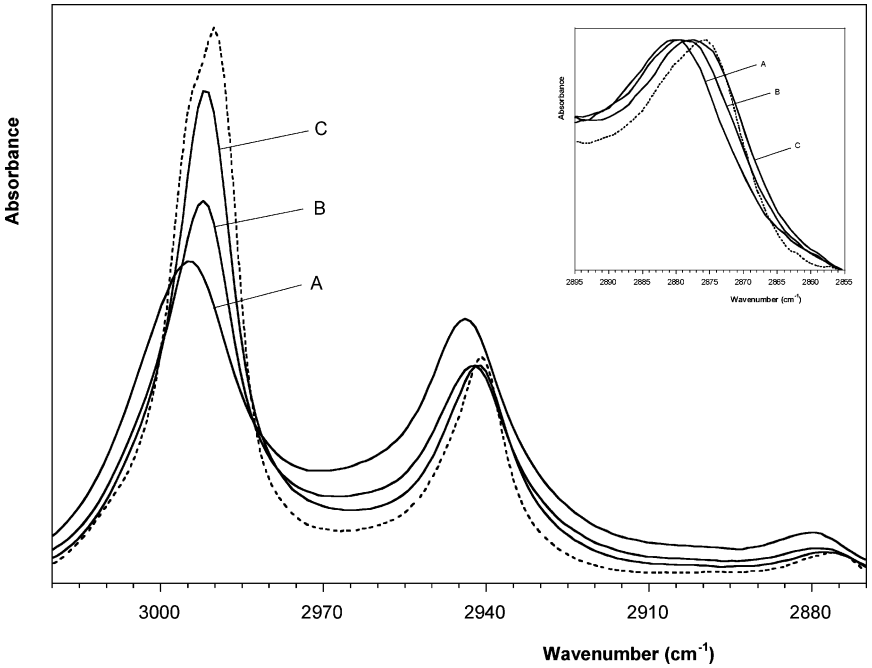

Figure 8. C−H stretching region of B50-50 recorded during isothermal crystallization at 190 °C, after melting at 240 °C for 2 min: (A) 0 min (amorphous blend); (B) after 30 min; (C) after 480 min. The spectrum obtained at room temperature after crystallization is highlighted with a dotted line. The autoscaled C_α−H stretching region is shown in the upper side square.

Taking into account the existence of two donor groups and a single acceptor site in the repetitive unit, the remaining question is how these interactions are spatially arranged. One possibility is the establishment of one to one hydrogen bonds in an alternate fashion. However, this arrangement is only possible within a unit cell of even number of repetitive units and is discarded because it has been reported that the racemic crystal of the PLLA/PDLA stereocomplex is formed by packing 3_1 helices of opposite absolute configuration.[16] The other possibility is the occurrence of multicentric C−H···O hydrogen bonds, a usual structure for this type of interactions, frequently observed in crystalline repetitive structures.[43] Thus, infrared results suggest a packing structure in which the carbonyl group of one of the isomers is located in front of the CH_3 and $C_\alpha H$ groups of the chiral carbon atom of its complementary isomer, hydrogen bonding with both groups. Molecular modeling calculations supporting this spatial arrangement are presented later in this paper. Finally, the stereocomplex spectra do not show Fermi resonance bands, and thus interchain CH_3 interactions can be discarded.

Temperature Dependence. Another interesting point regards the spectral shift observed in the C−H spectral region with temperature. Figure 9 displays the location of the $C_\alpha H$ stretching peak in the temperature range 30−190 °C. As can be seen, the location of the $C_\alpha H$ stretching band increases with temperature about 0.014 $cm^{-1}/°C$; thus, the spectral shift at 190 °C decreases to about half of its value at room temperature. Spectral shifts are usually related to the strength of the interactions, suggesting a gradual weakening of C−H···O hydrogen bonds as temperature is raised.[48] However, the C=O stretching band remains nearly unaltered, and a deeper discussion seems necessary.

The interaction of a X−H group with one of the lone pairs of the C=O oxygen atom increases the polarization of the $C^{\delta+}-O^{\delta-}$ bond; hence, the carbonyl bond becomes weaker and absorbs at lower wavenumbers.[55] In addition, stronger hydrogen bonds lead to higher polarizations; thus, the spectral shift in the C=O stretching band is usually accepted to reflect the strength of the interaction. In the case of B50-50, the negligible variation of the C=O stretching band location with temperature indicates that the inherent strength of the interaction, reflected by the polarization in the C=O group or by the depth of the minimum in the curve of interaction energy vs interatomic distance,[49] remains unaltered.

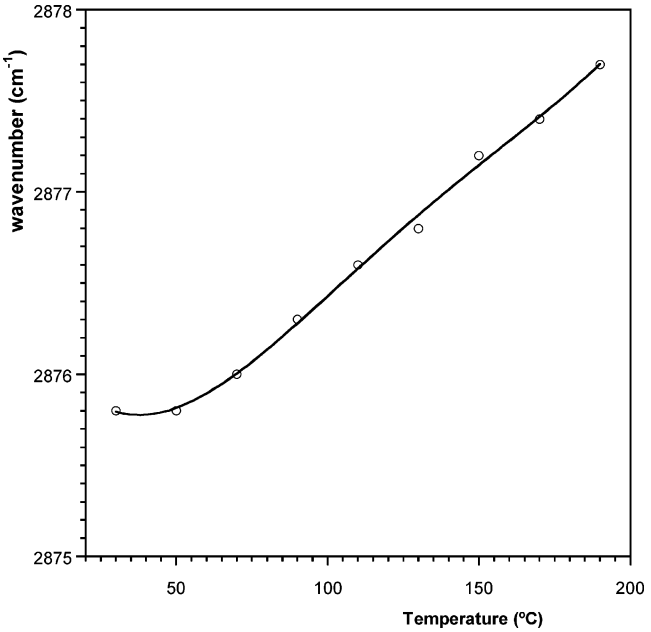

Figure 9. Location of the C_α−H stretching band with temperature.

In the C−H spectral region, the location of the C−H absorption band also reflects the strength of the C−H bond, but polarization issues are not a matter of concern. In this spectral region, as the strength of the hydrogen bond increases, the C−H bond becomes weaker, absorbing at lower wavenumbers. The strength of the

hydrogen bond is known to depend on its geometry, stronger bonds being formed as the linearity of the atomic arrangement increases and the hydrogen-bonding distance decreases.[43] The shift to higher wavelengths of the C−H stretching band as temperature increases can be attributed to higher thermal motion, resulting in longer interatomic distances or lateral displacements of the C−H group over a wider range of hydrogen-bonding angles. This effect can be better understood with the typical potential energy vs interatomic distance curves: an increase in thermal motion implies longer interaction distances, hence the attractive force exerted by the C=O group over the hydrogen atom in the C−H group is reduced, and thus the C−H bond becomes stronger, absorbing at higher wavenumbers.

In addition, the locations for the fundamental modes of the asymmetric CH_3 stretching band, 2989 and 2995 cm^{-1}, can be obtained at room temperature by second-derivative analysis. Thus, hydrogen bonding seems to reduce the energy difference between the two fundamental CH_3 asymmetric stretching modes to 6 cm^{-1}, compared to the value of 9 cm^{-1} found in PLLA. Finally, we do not observe any pseudo-CH_2 stretching band[37,48] in the whole C−H spectral region. Such assignments were performed in the C−H stretching region of poly(hydroxy butyrate)s, arguing that the involvement of one of the three C−H bonds of the methyl group in the C−H···O interaction would result in a vibrating group similar to a CH_2. In our opinion, this hypothesis is not reasonable because the hydrogen bond cannot behave as a covalent bond due to the high energetic difference.[52] We guess the origin of the reported "pseudo-CH_2" bands is probably found in traditionally accepted causes, such as Fermi resonance.

Molecular Modeling. FTIR results suggest a hydrogen-bonding structure that must be possible to arrange within the real crystal. The crystalline structure of the PLLA/PDLA stereocomplex has been reported by Brizzolara et al.,[16] and polylactide chains can be built according to reported RIS models,[39] based on results obtained in structural analysis of esters. To obtain a perfect 3_1 helix, dihedral angles were slightly modified, according to optimized values reported by Hirai et al.[57] Figure 10a shows a PLLA and a PDLA chain in parallel orientation, at the same relative distance than in the unit cell reported by Brizzolara.[16] According to accepted geometries for C−H···O hydrogen bonds,[43] possible interactions are indicated. The resulting hydrogen-bonding distance is of about 2.9 Å, and hydrogen bond angles are 120° for the C_α−H···O interaction and 150° for the CH_3···O hydrogen bond. Note that both hydrogen-bonding angles are above the accepted cutoff angle (110°).[43] These geometries support our IR resuts, as the suggested C_α−H···O and CH_3···O interactions in an alternate fashion are geometrically possible.

The crystal lattice built by packing the helical chains in Figure 10a is displayed in Figure 10b. As can be seen, the obtained crystalline structure resembles that reported by Brizzolara.[16] However, they reported van der Waals interactions between opposite oxygen atoms and hydrogen atoms.[16] Our results indicate that we should properly talk about C−H···O hydrogen bonds. Interactions between PLLA and PDLA in the unit cell occur pairwise, each oxygen atom being hydrogen bonded with two hydrogen atoms of its enantiomeric chain.

Strength of the Interactions. The strength of the interactions can be estimated from known empirical correlations for both the C=O and C−H stretching regions. A similar value obtained from both spectral regions should indicate a direct correlation between these interacting groups. Brown et al.[51] found a linear $\Delta H-\Delta\nu_{C=O}$ relation for ethyl acetate adducts, and eq 4 can be obtained by least-squares fitting of the data tabulated in their work:

$$-\Delta H_f = 0.123\Delta\nu \tag{4}$$

where $\Delta\nu$ is in cm^{-1} and ΔH_f in kcal/mol. Polymers also fit adequately this equation, as can be tested by comparing calculated values with experimental data obtained from well-known hydrogen-bonded polymer systems.[52] For the formation of stereocomplex crystals, the red shift of about 8 cm^{-1} results in $\Delta H_f = 1.0$ kcal/mol. The value corresponding to each hydrogen bond is 0.5 kcal/mol, reflecting weak interactions, but the duplicate nature of the hydrogen bond gives a total value in the frontier of weak to moderate interactions.

The result obtained in the C=O stretching region can be compared to that obtained for the C−H stretching region. Good correlations between spectral shift and intensity[53] or between spectral shift and interatomic distance[50] have been verified for a wide range of interacting systems. However, the correlation between spectral shift and interaction energy is lost especially in weak hydrogen bonds,[50,53] and the relation proposed by Rozenberg et al. should be taken with caution in systems with interaction energy below 2.4 kcal/mol:[50]

$$-\Delta H_f = 1.3(\Delta\nu)^{1/2} \tag{5}$$

where ΔH_f is in kJ/mol and $\Delta\nu$ is in cm^{-1}. Assuming multicentric interactions (each C=O bonds to one CH_3 and one $C_\alpha H$ group) and a spectral shift of 4 cm^{-1}, a tentative calculation results in a hydrogen-bonding enthalpy $\Delta H_f = 2 \times 1.3 \times (4)^{1/2} = 5.2$ kJ/mol (1.2 kcal/mol).

A good agreement is found between the values calculated from the C=O and C−H stretching spectral regions, considering the estimative character of $\Delta\nu-\Delta H$ relations. The mean enthalpy of hydrogen bonding, 1.1 kcal/mol, is about 4 times higher than reported,[20] within the characteristic range of weak to moderate interactions. This value is also in good agreement with a rough estimation based on ab initio calculations. The interaction energy at the MP2/6-31+G** level for similar interacting groups (H_3CH····$O{=}CH_2$),[49] is 0.37 kcal/mol, within the typical range for C−H····O hydrogen bonds established by carbon atoms with sp^3 hybridization.[44] In addition, cooperativity is known to increase the strength of the interactions by about a 25% for weak interacting systems.[54] Hence, a value of about 0.9 kcal/mol results from this rough estimation, in good agreement with the experimental value. The reader should be aware that this kind of estimation must be taken with great caution because it is based on systems of completely different geometry to the one studied in this work. For the low molecular weight system cited in this paragraph, the hydrogen-bonding distance is higher (3.8 Å), but the interaction angle is mostly linear (180°).

Conclusions

Stereoselective crystallization conditions for polylactides have been found by annealing of stoichiometric

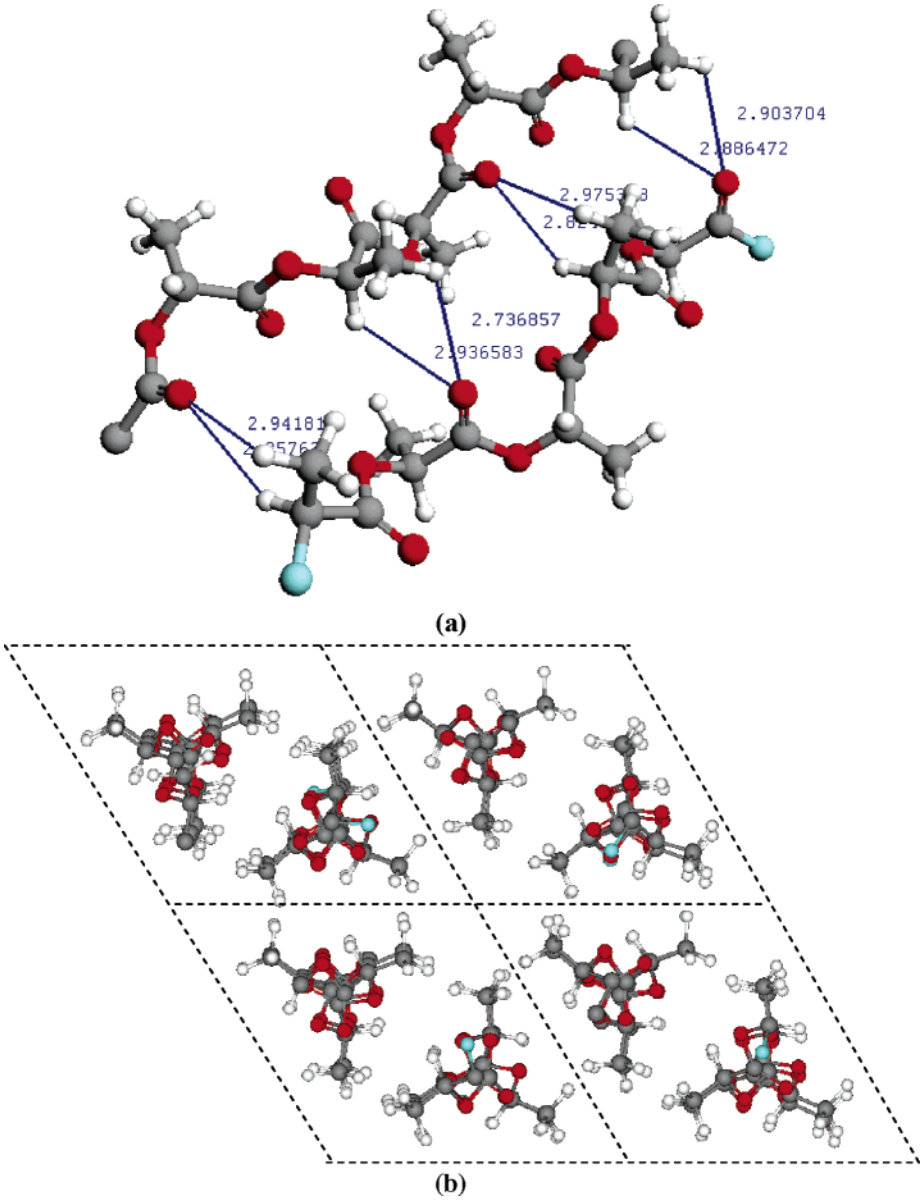

Figure 10. (a) PDLA (top) and PLLA (bottom) chains in parallel orientation, as located in the stereocomplex crystal. Chains have been approximated until fitting in the experimental dimensions of the unit cell. Hydrogen-bonding angles for the interactions suggested by FTIR are 120° and 150° for $C_\alpha-H\cdots O$ and $CH_3\cdots O$ bonds, respectively, and hydrogen bond distance is about 2.9 Å. (b) Stereocomplex crystal lattice built from chains in the arrangement proposed.

PLLA/PDLA blends at different temperatures. DSC and XRD studies provided evidence of a favorable α form crystal structure at annealing temperatures below 180 °C. However, at annealing temperatures close to the melting of α crystals, stereocomplex crystals were exclusively formed.

Crystallization of the polylactide stereocomplex crystalline structure resulted in an increase of melting temperature of about 50 °C with respect to that obtained in homocrystalline samples. XRD patterns of stereocomplexed polylactides revealed a more compact crystalline structure, and FTIR results provided a new band at 1748 cm^{-1}, attributed to crystalline polylactide chains in the 3_1 helical conformation.

In polylactides, conformation has been found to influence absorption wavenumbers due to coupling between C=O groups along the lactide chain. This influence can be accounted for,[39] and the absorption wavenumber expected for the E mode of the carbonyl stretching band of a polylactide in 3_1 helical conformation is 1756 cm^{-1}. Hence, a spectral shift of 8 cm^{-1} is found in the C=O spectral region. In addition, the spectral bands attributed to the interlamellar material indicate a truly amorphous phase, in contrast with the semiordered interphase found during crystallization of PLLA. Hence, crystallization mechanisms of PLLA and the stereocomplex are revealed different.

Crystallization of PLLA shows only subtle changes in the C−H spectral region. In the case of the stereocomplex, a red shift of about 2 cm^{-1} is observed for both the CH_3 and $C_\alpha H$ stretching regions during crystallization, which increases to 4 cm^{-1} after cooling to room temperature. These spectral changes suggest an arrangement for the hydrogen bonds in the form of multicentric interactions. (Each C=O group hydrogen bonds with one hydrogen atom from the CH_3 group and the $C_\alpha H$ hydrogen atom.) The C−H stretching band shifts with temperature, reflecting an increase in the hydrogen-bonding distance due to higher thermal energy. However, the C=O stretching band location re-

mains unaltered, reflecting a nearly constant interaction energy vs interatomic distance dependence.

Molecular modeling results support the hydrogen-bonding arrangement deduced by FTIR results. Hydrogen-bonding angles for the $C_\alpha-H\cdots O$ and $CH_3\cdots O$ are found to be respectively 120° and 150°, and the interaction distance is found to be 2.9 Å. Finally, the strength of the interactions has been calculated from both the C=O and C−H spectral regions. A good agreement has been found, resulting in a mean value of 1.1 kcal/mol. This value is also close to that expected according to ab initio calculations.

Acknowledgment. The authors are thankful for financial support from the Basque Government—Dpt. of Industry, Trade and Tourism (Project IE03-105)—and the University of Basque Country EHU-UPV (Project 1/UPV 00151.345-T-15625/2003). They also acknowledge the collaboration of other members of CIC biomaGUNE and the support from the BIOBASK Agency.

References and Notes

(1) De Santis, P.; Kovacs, A. J. *Biopolymers* **1968**, *6*, 299.
(2) Okihara, T.; Tsuji, M.; Kawaguchi, A.; Katayama, K.; Tsuji, H.; Hyon, H.; Ikada, Y. *J. Macromol. Sci., Phys.* **1991**, *B30*, 119.
(3) Ikada, Y.; Jamshidi, H.; Tsuji, H.; Hyon, S. *Macromolecules* **1987**, *20*, 904.
(4) Bosscher, F.; ten Brinke, G.; Challa, G. *Macromolecules* **1982**, *15*, 1442.
(5) Koennecke, K.; Rehage, G. *Makromol. Chem.* **1983**, *184*, 2679.
(6) Matsubayshi, H.; Chatani, Y.; Tadokoro, H.; Dumas, P.; Spassky, N.; Gigwalt, P. *Macromolecules* **1977**, *10*, 996.
(7) Sakakihara, H.; Takakashi, Y.; Tadokoro, H.; Oguni, N.; Tani, H. *Macromolecules* **1973**, *6*, 205.
(8) Grenier, D.; Prud'homme, R. E.; Leborgne, A.; Spassky, N. *J. Polym. Sci., Polym. Phys. Ed.* **1984**, *22*, 577.
(9) Lavallée, C.; Prud'homme, R. E. *Macromolecules* **1989**, *22*, 2438.
(10) Murdoch J.-R.; Loomis, G.-L. US Patent 4719246, 1988; US Patent 4766182, 1988; US Patent 4800219, 1989.
(11) Bostman, O. M. *J. Bone Jt. Surg.* **1991**, *73-A*, 148.
(12) Sinclair, R. G. *J. Macromol. Sci., Pure Appl. Chem.* **1996**, *A33*, 587.
(13) Södegard, A.; Stolt, M. *Prog. Polym. Sci.* **2002**, *27*, 1123.
(14) Garlotta, D. *J. Polym. Environ.* **2001**, *9*, 63.
(15) Tsuji, H.; Ikada, Y. *Macromol. Chem. Phys.* **1996**, *197*, 3483.
(16) Brizzolara, D.; Cantow, H.-J.; Diederichs, K.; Keller, E.; Domb, A. *Macromolecules* **1996**, *29*, 191.
(17) Zhang, J.; Tsuji, H.; Noda, I.; Ozaki, Y. *Macromolecules* **2004**, *37*, 6433.
(18) Kang, S.; Aou, K.; Pekrul, R. L.; Hsu, S. L. *Polym. Prepr.* **2002**, *43*, 894.
(19) Tretinnikov, O. N. *Macromolecules* **2003**, *36*, 2179.
(20) Zhang, J.; Sato, H.; Tsuji, H.; Noda, I.; Ozaki, Y. *Macromolecules*, in press.
(21) Schindler, A.; Harper, D. H. *J. Polym. Sci., Polym. Chem. Ed.* **1979**, *17*, 2593.
(22) Savitzky, A.; Golay, M. J. E. *Anal. Chem.* **1964**, *36*, 1627.
(23) Steiner, J.; Termonia, Y.; Deltour, J. *Anal. Chem.* **1972**, *44*, 1906.
(24) Meaurio, E.; Zuza, E.; Sarasua, J. R. *Macromolecules* **2005**, *38*, 1207.
(25) Loomis, G. L.; Murdoch, J. R.; Gardner, K. H. *Polym. Prepr.* **1990**, *31*, 55.
(26) Tsuji, H.; Ikada, Y. *Macromolecules* **1993**, *26*, 6918.
(27) Sarasua, J. R.; Prud'homme, R. E.; Wisniewski, M.; Le Borgne, A.; Spassky, N. *Macromolecules* **1998**, *31*, 3895.
(28) Sarasua, J. R.; López Arraiza, A.; Balerdi, P.; Maiza, I. *J. Mater. Sci.* **2005**, *40*, 1855.
(29) Kalb, B.; Pennings, A. J. *Polymer* **1980**, *21*, 607−612.
(30) Eling, B.; Gogolewski, S.; Pennings, A. J. *Polymer* **1982**, *23*, 1587.
(31) Sawai, D.; Takahashi, K.; Aki, S.; Kenamoto, T.; Hyon, S.-H. *Macromolecules* **2003**, *36*, 3601.
(32) Cartier, L.; Okihara, T.; Ikada, Y.; Tsuji, H.; Puiggali, J.; Lotz, D. *Polymer* **2000**, *41*, 8909.
(33) Tsuji, H.; Hyon, S. H.; Ikada, Y. *Macromolecules* **1991**, *24*, 5651.
(34) Kister, G.; Cassanas, G.; Vert, M. *Polymer* **1998**, *39*, 267.
(35) Kang, S.; Hsu, S. L.; Stidham, H. D.; Smith, P. B.; Leugers, M. A.; Yang, X. *Macromolecules* **2001**, *34*, 4542.
(36) Zhang, J.; Tsuji, H.; Noda, I.; Ozaki, Y. *J. Phys. Chem. B* **2004**, *108*, 11514.
(37) Zhang, J.; Sato, H.; Tsuji, H.; Noda, I.; Ozaki, Y. *J. Mol. Struct.* **2005**, *735*, 249.
(38) Tam, C. N.; Bour, P.; Keiderling, T. A. *J. Am. Chem. Soc.* **1996**, *118*, 10285.
(39) Meaurio, E.; Zuza, E.; López, N.; López, A.; Sarasua, J. R. Submitted for publication.
(40) Brant, D. A.; Tonelli, A. E.; Flory, P. J. *Macromolecules* **1969**, *2*, 228.
(41) Lagaron, J. M. *Macromol. Symp.* **2002**, *184*, 19.
(42) Allerhand, A.; Schleyer, P. R. *J. Am. Chem. Soc.* **1963**, *85*, 1715.
(43) Desiraju, G. R. *Acc. Chem. Res.* **1996**, *29*, 441.
(44) Scheiner, S.; Grabowski, S. J.; Kar, T. *J. Phys. Chem. A* **2001**, *105*, 10607.
(45) Steinfeld, J. I. *Molecules and Radiation*: *An Introduction to Modern Molecular Spectroscopy*, 2nd ed.; M.I.T. Press: Cambridge, MA, 1993.
(46) MacPhail, R. A.; Strauss, H. L.; Snyder, R. G.; Elliger, C. A. *J. Phys. Chem.* **1984**, *88*, 334.
(47) Snyder, R. G.; Strauss, H. L.; Elliger, C. A. *J. Phys. Chem.* **1982**, *86*, 5145.
(48) Sato, H.; Murakami, R.; Padermshoke, A.; Hirose, F.; Senda, K.; Noda, I.; Ozaki, Y. *Macromolecules* **2004**, *37*, 7203.
(49) Gu, Y.; Kar, T.; Scheiner, S. *J. Am. Chem. Soc.* **1999**, *121*, 9411.
(50) Rozenberg, M.; Loewenschuss, A.; Marcus, Y. *Phys. Chem. Chem. Phys.* **2000**, *2*, 2699.
(51) Brown, D. G.; Drago, R. S.; Bolles, T. F. *J. Am. Chem. Soc.* **1968**, *90*, 5706.
(52) Coleman, M. M.; Graf, J. F.; Painter, P. C. *Specific Interactions and the Miscibility of Polymer Blends*; Technomic Publishing Inc.: Lancaster, PA, 1991.
(53) Iogansen, A. V. *Spectrochim. Acta, Part A* **1999**, *55*, 1585.
(54) Kar, T.; Scheiner, S. *J. Phys. Chem. A* **2004**, *108*, 9168.
(55) Paoloni, L.; Patti, A.; Mangano, F. *J. Mol. Struct.* **1975**, *27*, 123.
(56) ArgusLab 4.0**,** Thompson, M. A.**,** mark@arguslab.com, Planaria Software LLC, Seattle, WA, http://www.arguslab.com.
(57) Hirai, Y.; Nakajima, T. *J. Macromol. Sci., Phys.* **1991**, *B30*, 141.

MA051266Z